A Spectroscopic Investigation of the Conformational Dynamics of Insulin in Solution†

Isaiah Pittman IV*,‡ and Howard S. Tager§

Department of Biochemistry and Molecular Biology, The University of Chicago, Chicago, Illinois 60637

Received December 21, 1994; Revised Manuscript Received May 9, 1995⊗

ABSTRACT: A conformational change, termed the T → R transition, which can be detected by visible, circular dichoric, and fluorescence spectroscopy, occurs in native insulin and tryptophan substituted insulin analogs ([Trp^{B25}]-, [Trp^{B26}]-, [Gly^{B24},Trp^{B25}]-, and [Gly^{B24},Trp^{B26}]insulin) upon binding specific alcohol ligands, including phenol and cyclohexanol. In these studies we have demonstrated that changes in the visible absorbance spectrum of an insulin$_6(Co^{2+})_2$ solution are not a definitive means of determining the occurrence of T → R transitions in the presence of alcohol ligands. We also have presented evidence that fast protein liquid chromatography (FPLC) can be used to determine the aggregation state of insulin and that *des*-octapeptide(B23−30)insulin (DOI) forms Zn^{2+}-coordinated hexamers that appear to be stabilized by the T → R transformation. Using fluorescence spectroscopy, we have shown that in the presence of specific alcohol ligands the B-chain COOH-terminal residues, particularly position B25, of hexameric, as well as monomeric insulin undergo a conformational change which appears to be related to the T → R transformation. Circular dichroic studies indicate that a conformation similar to the R-state of metal-coordinated hexameric insulin can be induced by binding cyclohexanol; however, this new conformational state (R_I-state) exists independent of divalent metal ion coordination, and therefore of hexamer formation. We further show that monomeric insulin can be induced to assume the R_I-state upon alcohol binding, therefore illustrating the first defined conformational change described for monomeric insulin. We suggest that this new conformation may be an intermediate state in the T → R transformation in metal-coordinated hexameric insulin, such that T → R_I → R. The model presented here of the structural adjustments undergone by insulin upon binding cyclohexanol provides further insight into the conformational flexibility of insulin in solution.

Insulin (MW ≈ 5800) is a disulfide linked heterodimer in which the A-chain (21 residues) and the B-chain (30 residues) are linked at positions A7−B7 and A20−B19. There is also an internal disulfide link in the A-chain from Cys^{A6} to Cys^{A11}. In spite of its small size, insulin maintains a defined secondary structure which has been determined by X-ray crystallography and 2D-NMR of hexameric complexes of insulin, and of monomeric insulin, respectively (Blundell et al., 1972; Baker et al., 1988; Hua & Weiss, 1991; Weiss et al., 1991). In the β-cells of the pancreas, insulin is stored as hexamers, coordinated by the divalent metal ions Zn^{2+} and Ca^{2+}. As insulin leaves the β-cells and enters the blood, its concentration drops drastically, to within 10^{-9}−10^{-11} M, which allows the hexameric complexes to dissociate and the monomeric form of the molecule to exist in the plasma (Goldman & Carpenter, 1974) and bind to insulin receptors on the plasma membrane of cells. The K_D of insulin for its receptor is in the nanomolar range ($K_D \approx 10^{-9}$ M), and many analogs have been constructed which display increased or decreased binding affinity in attempts to determine how insulin interacts with its receptor (Mirmira & Tager, 1989; Schwartz et al., 1989; Nakagawa & Tager, 1991; Shoelson et al., 1993). Abnormal insulins, as the result of genetic mutations in man, have also been investigated to determine structure−function relationships. Three mutated human insulins with little biological activity are insulin Chicago (Phe^{B25} → Leu), insulin Los Angeles (Phe^{B24} → Ser), and insulin Wakayama (Val^{A3} → Leu) [cf. Tager (1990a)]. All of these genetically mutated insulins have ≤1% receptor binding affinity.

The crystal structure of 2-Zn insulin has been solved to 1.5 Å and provides an excellent model of insulin in hexameric coordination (Blundell et al., 1972; Baker et al., 1988). The hexamer consists of three dimeric units and possesses a 3-fold symmetry axis. In this structure, the N-terminus of the B-chain (B1−8) is in an extended conformation, residues B9−19 are α-helical, residues B20−22 are involved in a β-turn, and B23−30 form a β-strand that interacts with the central helix to complete the characteristic insulin fold (T-state). The carboxy-terminal B-chain residues also form an antiparallel β-sheet structure between two monomers in a dimeric unit. The dimeric unit is asymmetric and displays Phe^{B25} in two different orientations: the molecule I orientation in which Phe^{B25} is inward, adjacent to the hydrophobic core of its respective monomer; and molecule II where Phe^{B25} is outward, crossing the dimer

† These studies were supported by Grants DK 18347 and DK 20595 from the National Institutes of Health.

* Address correspondence to this author at the Department of Biochemistry and Molecular Biology, The University of Chicago, 920 E. 58th St., Chicago, IL 60637. Telephone: (312) 702-1345; Fax: (312) 702-0439.

‡ Recipient of the Institutional Training Grant in Growth and Development HD-07009-20 from the National Institutes of Health, and the National Medical Fellowship from Bristol-Myers Squibb.

§ This paper, and the work that emanates from it, is dedicated to Dr. Howard S. Tager, Ph.D. (1945−1994), in appreciation for his unequivocal guidance as a mentor and contributions to the field of Biochemistry, particularly concerning insulin structure and function.

⊗ Abstract published in *Advance ACS Abstracts,* August 1, 1995.

0006-2960/95/0434-10578$09.00/0

interface. It was later found, using 2D-NMR, that the conformation of monomeric insulin in solution is virtually the same as the crystal structure (Hua & Weiss, 1991; Weiss et al., 1991). Mini-proinsulin (Markussen et al., 1985), which is an insulin analog containing an α-carboxy Lys^{B29} to α-amino Gly^{A1} amide cross-link, was also crystallized and was found to have a conformation practically identical to that of the T-state; however, the receptor binding affinity of mini-proinsulin is extremely low (<0.1%). Based on these findings, it was speculated that the T-state, more than likely, is not the conformation of insulin which binds to receptor (Derewenda et al., 1991; Hua et al., 1992, 1993).

Subsequently, insulin in hexameric coordination was found to undergo a conformational adjustment in which the N-terminus of the B-chain (B1−8) changes from an extended conformation (T-state) to an α-helical conformation (R-state) in the presence of phenol, and other cyclic alcohol ligands (Derewenda et al., 1989; Smith & Dodson, 1992; Smith & Ciszak, 1994). Crystallographic studies demonstrated that this change not only causes a readjustment in secondary structure, but also causes a 25 Å translational movement of the N-terminus of the B-chain, as well as a slight separation of the B-chain COOH-terminal β-strand from the central B-chain helix (Dodson et al., 1983). Interestingly, the COOH-terminal region of insulin B-chain has long been the subject of intensive study and is relevant to both insulin structure and insulin−receptor interactions [Nakagawa & Tager, 1986; cf. Steiner et al. (1990); cf. Tager (1990a)]. Monovalent anions, such as SCN^- and Cl^-, have been found to stabilize the R_6-state of insulin in the presence of phenol-like molecules and induce a T_3R_3 hexameric state in the absence of an alcohol ligand (Cutfield et al., 1981; Chothia et al., 1983). In the T_3R_3 hexamer the dimeric unit consists of one T-state and one R-state (B1−8 α-helix) insulin molecule coordinated by four Zn^{2+} ions (4-Zn insulin). Another T_3R_3 crystal structure has been solved which is similar to the previous structure except for the absence of a complete B1−8 helical structure in the R-state molecules (Ciszak & Smith, 1994). In this structure B1−3 is not α-helical but is extended.

The $T_6 \rightarrow R_6$ conformational transition has been found to cause the metal coordination center of hexameric insulin to change from an octahedral to tetrahedral arrangement (Derewenda et al., 1989). This change in coordination can be observed by means of visible spectroscopy when Co^{2+} is the coordinating metal (Roy et al., 1989). A solution of insulin$_6(Co^{2+})_2$ displays an increase in absorbance in the presence of phenol; the subsequent addition of monovalent anions results in a further increase in the absorbance maximum. Accordingly, circular dichroic spectra show an increase in negative ellipticity when the R-state is achieved, consistent with an increase in α-helical content (Wollmer et al., 1987, 1989). Therefore, CD, as well as visible absorbance, has been used extensively to analyze $T \rightarrow R$ structural transitions; however, monitoring the change in Co^{2+} coordination using visible spectroscopy is currently the most widely used technique for determining $T \rightarrow R$ conformational transitions. The $T \rightarrow R$ transition demonstrates the great structural variability of insulin and warrants further investigation of the conformational dynamics of this peptide hormone in order to assess the possible relevance of this structural transition. In the experiments presented here we have examined structural adjustments in hexameric, dimeric, and monomeric insulin. In doing so, (a) we have demonstrated that an alternate conformation of monomeric insulin can be induced that is similar, but not identical, to the hexameric R-state; and (b) we suggest that this conformational change may be involved in insulin−receptor interactions.

MATERIALS AND METHODS

Materials. Procine insulin and [[^{125}I]iodo-Tyr^{A14}]insulin were obtained from Calbiochem and DuPont NEN Research Products (Boston, MA), respectively. Tosylphenylalanine chloromethyl ketone (TPCK)[1]-treated trypsin was from Worthington (Freehold, NJ).

Preparation of Insulin Analogs with Altered B-Chain COOH-Terminal Domains. Each insulin analog was prepared by trypsin-catalyzed peptide bond formation between the α-carboxy group of Arg^{B22} of $(Boc)_2$-DOI and the α-amino group of an octapeptide (Inouye et al., 1981). The octapeptides were synthesized via solid phase methods previously described (Mirmira et al., 1991). $(Boc)_2$-DOI (1 μmol) and octapeptide (4 μmol) were incubated with TPCK-treated trypsin (0.3 mg) in a mixture of DMF/1,4-butanediol/0.2 M Tris acetate (pH 8, containing 10 mM calcium acetate and 1 mM EDTA) in the ratio 35:35:30 v/v (100 μL) at 12 °C for 24−72 h (Morihara et al., 1986; Nakagawa & Tager, 1993). The condensation yields (judged by analytical HPLC on a C-18 column in a solvent system of 0.1 M phosphoric acid/0.05 M triethylamine (adjusted to pH 3.0 with sodium hydroxide) and acetonitrile) were 30−50%. The Boc groups were then removed by trifluoroacetic acid (TFA) for all of the analogs except [Gly^{B24},Trp^{B25}]insulin, in which the Boc group was removed after purification. The analogs were then dissolved in 3 M acetic acid and purified via preparative HPLC on a C-4 column by use of a 0.1% aqueous TFA and 0.1% TFA in acetonitrile solvent system. The purified product was desalted on a Bio-Gel P-4 gel filtration column using 3 M acetic acid, collected, and lyophilized. The analogs were then dissolved in 0.1 M Tris brought to pH 7.6 by the addition of perchloric acid, and solutions were made to the desired concentrations using extinction coefficients calculated from the values $\epsilon_{Tyr}^{275} = 1340$ and $\epsilon_{Trp}^{275} = 5500$. The value $A_{275}^{mg/mL} = 1.86$ was calculated for [Trp^{B26}]- and [Gly^{B24},Trp^{B26}]insulin; and $A_{275}^{mg/mL} = 2.1$ for [Trp^{B25}]- and [Gly^{B24},Trp^{B25}]insulin. Porcine insulin concentrations were determined using $A_{275}^{mg/mL} = 1.05$ (Frank & Veros, 1968).

Receptor Binding Studies. Procedures for the isolation of canine hepatocytes and their use for receptor binding studies have been described previously (Bonnevie-Nielsen et al., 1982; Nakagawa & Tager, 1986). Cells (2×10^6/mL) of 98% viability were incubated with [[^{125}I]iodo-Tyr^{A14}]insulin plus selected concentrations of insulin or insulin analogs (determined via UV absorbance) for 30 min at 30 °C.

Fluorescence Studies. Fluorescence spectra were recorded on a PTI fluorimeter interfaced with an NEC computer, using

[1] Abbreviations: TPCK, tosylphenylalanine chloromethyl ketone; Boc, (*tert*-butyloxy)carbonyl; DMF, dimethylformamide; TFA, trifluoroacetic acid; HPLC, high performance liquid chromatography; FPLC, fast protein liquid chromatography; DOI, *des*-octapeptide(B23−30)-insulin; CD, circular dichroism; EDTA, ethylenediaminetetraacetic acid; $(Boc)_2$-DOI, N^{α}-Gly^{A1},N^{α}-Phe^{B1}-bis-Boc-*des*-octapeptide(B23−30)-insulin; NAWEE, *N*-acetyltryptophan ethyl ester.

a 0.8 mL sample cell with a 1 cm path length. Fluorescence emission scans were taken from 310 to 450 nm, while exciting at 295 nm. An average of three runs was used for each of the final spectra; and all background effects were subtracted to obtain spectra representative of changes in the environment of the substituted tryptophan in the insulin analogs. All solutions were in 0.1 M Tris/ClO_4^- buffer at pH 7.6 and were at concentrations of 1−4 μM, at which native insulin is monomeric. Fluorescence quenching studies were performed using acrylamide as a quenching agent. Inner filter effects were determined using the equation: $F_{corr} = F_0(A_{ex} + A_{em})/2$, where F_{corr} is the corrected fluorescence emission value and F_0 is the original fluorescence (Lakowicz, 1983a), and were found to be minimal when the absorbance of acrylamide was observed at the excitation (A_{ex}), and emission (A_{em}), wavelengths used in these experiments. All of the data from the fluorescence quenching studies were modeled using the modified Stern−Volmer equation (Eftink & Ghiron, 1976): $F_0/F = (1 + K_{sv}[Q])e^{V[Q]}$, where [Q] is the concentration of acrylamide used, and K_{sv} and V are the Stern−Volmer (dynamic) and static quenching constants, respectively.

Circular Dichroic Studies. CD spectra were recorded on a Jasco Model J600 spectropolarimeter interfaced with an IBM PC XT computer. CD spectra for all samples were measured in 0.1 M Tris/ClO_4^- buffer at pH 7.6, with insulin concentrations determined using $A_{275}^{mg/mL} = 1.05$ on a Beckman DU-40 spectrophotometer. All studies were conducted using a 0.1 mm cell path length, and the final spectra obtained from an average of six scans. Backgrounds were subtracted and spectra were converted to molecular ellipticity based on mean residual weight (MRW = 113).

Visible Studies. Visible spectra of the T → R structural transitions of insulin$_6(Co^{2+})_2$ complexes (transitions that are induced by phenol-like compounds and are stabilized by chloride anions) were examined by methods described previously (Roy et al., 1989; Thomas & Wollmer, 1989; Nakagawa & Tager, 1991). Visible spectra were recorded for insulin dissolved in 0.1 M Tris/ClO_4^- buffer at pH 7.6 on a Beckman DU-40 spectrophotometer using a 1 cm cell.

FPLC Column Elution Studies. The state of aggregation of insulin and insulin analogs was assessed by gel permeation plateau chromatography (Valdes & Ackers, 1979) using a Perkin-Elmer Series 4 HPLC with a LC 135 diode array detector and LCI 100 laboratory computing integrator. Six milliliters of insulin in buffer was loaded onto a Pharmacia Superdex-75 FPLC column equilibrated with the same buffer. The use of this large volume of sample assured that the leading edge of the chromatographic peak would correspond to that of the predominant aggregate species in the mixture. This leading edge should be followed by a plateau, the height of which reflects the concentration of the injected sample. The plateau also assures that the leading portion of the peak is at a uniform concentration, reflecting a uniform state of aggregation. For the elution studies using insulin analogs, fractions were collected at 1.33 min/tube for fluorescence analysis.

RESULTS

Changes in Co^{2+} Coordination vs Changes in Conformation. Several alcohol ligands, including phenol and cyclohexanol, induce the T → R transition (Brader et al., 1991).

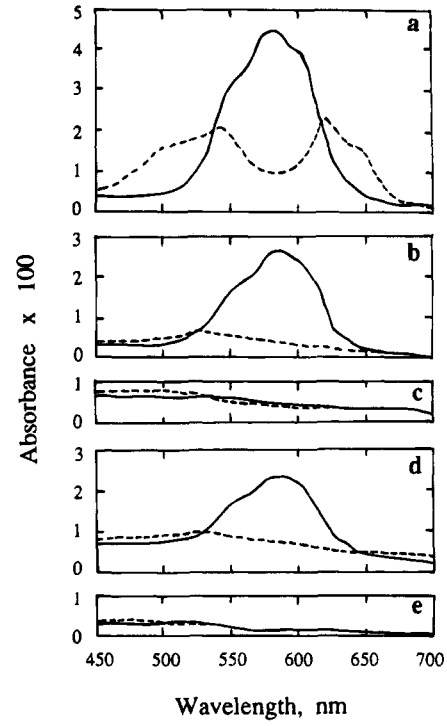

FIGURE 1: Spectroscopic studies of T → R transition in insulin Co^{2+} hexamers. In all of the panels, 1.45 mg/mL porcine insulin, in 0.1 M Tris/ClO_4^- buffer at pH 7.6, was incubated with 0.17 mM $CoCl_2$. The dashed lines represent the absorbance spectra of insulin$_6(Co^{2+})_2$ complexes in the presence of (a) 100 mM phenol, and 360 mM (b) cyclohexanol, (c) cyclopentanol, (d) 3-pentanol, and (e) 2-propanol. The solid line of each spectrum illustrates the absorbance of the insulin hexamers in the presence of their respective alcohol ligand with 250 mM NaCl.

In addition to phenol and cyclohexanol, 3-pentanol, cyclopentanol, and 2-propanol were assessed for their ability to change the coordination of Co^{2+} in hexameric insulin from octahedral to tetrahedral, which has previously been shown to be associated with the T → R transition (Roy et al., 1989; Thomas & Wollmer, 1989). The additional aliphatic alcohols might be preferable to phenol, since these ligands lack aromatic rings which would interfere with subsequent fluorescence studies. Figure 1 demonstrates the effects of the different alcohols and Cl^- anion on the visible spectrum of Co^{2+} in hexameric complexes of insulin. In the presence of a stabilizing anion, phenol has the greatest effect, causing the largest increase in the absorbance spectrum from 550 to 650 nm, consistent with the T → R conformational change. Cyclohexanol and 3-pentanol also increase the absorbance of Co^{2+}-coordinated hexameric insulin in the presence of 250 mM Cl^-; cyclopentanol and 2-propanol, however, display no change in absorbance under the given conditions.

The above findings suggest that 3-pentanol, an unbranched aliphatic chain, induces the R-state. Circular dichroic studies were conducted to determine if, in fact, the binding of the selected alcohol ligands causes an increase in α-helix content (T → R transformation) in a solution of insulin. Figure 2 demonstrates that the alcohol ligands increased the α-helical content of insulin, indicative of the R-state, in the following order of effectiveness: cyclohexanol ≈ 3-pentanol > cyclopentanol ≫ 2-propanol ≈ insulin in the absence of an alcohol ligand. The increased negative ellipticity of Zn^{2+}-coordinated insulin hexamers in the presence of cyclopentanol and Cl^- (Figure 2c) indicates that cyclopentanol causes

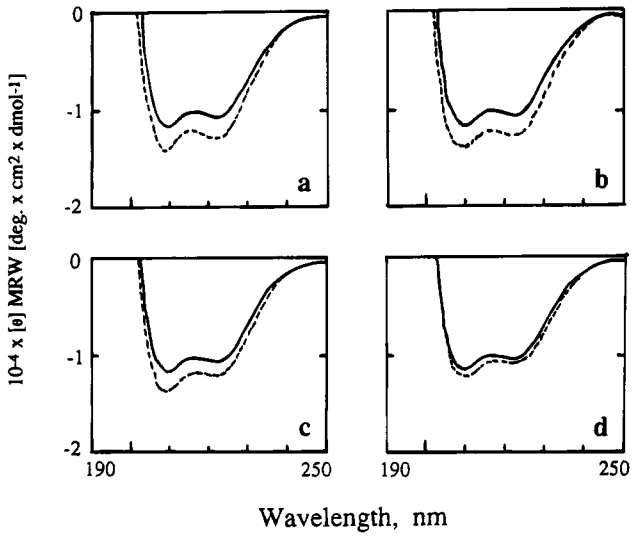

FIGURE 2: Determination of α-helix formation using circular dichroism. Panels a–d illustrate the CD spectra of 2.9 mg/mL insulin in the presence of 0.17 mM $ZnSO_4$ and 250 mM NaCl (solid line) in 0.1 M Tris/ClO_4^- buffer at pH 7.6. The dashed line represents the ellipticity changes, based on mean residual weight, due to the addition of 360 mM alcohol ligand: (a) cyclohexanol, (b) 3-pentanol, (c) cyclopentanol, and (d) 2-propanol, to the above-mentioned solution.

the T → R conformational transition. In contrast, the visible spectra reported above showed no change upon the addition of cyclopentanol to insulin hexamers. These results suggest that an increase in α-helix content—the hallmark of the R-state—can occur without a concomitant change in the visible spectrum, nor, by inference, a change in Co^{2+} coordination; or that Co^{2+}-coordinated hexamers may not be capable of undergoing the T → R transition under similar conditions as Zn^{2+} hexamers.

Circular dichroic studies were subsequently conducted using Co^{2+}, instead of Zn^{2+}, and demonstrated that Co^{2+}-coordinated hexamers also display an increase in α-helix in the presence of cyclopentanol and Cl^- (data not shown). Therefore, it appears as though Co^{2+} hexamers can, in fact, assume an R-state conformation in the absence of tetrahedral coordination. Previous crystallographic studies have indicated that there is no space for the R-state in an octahedrally coordinated hexamer (Smith & Dodson, 1992; Ciszak & Smith, 1994); however, Wollmer et al. (1987) have demonstrated that insulin in Ni^{2+}-coordinated hexamers, which cannot assume a tetrahedral coordination, can sustain an incomplete R-state. These studies indicate that such an R-state may exist in Co^{2+}-coordinated hexamers in the presence of cyclopentanol and Cl^-.

Fluorescence Tracing of Hexameric Complexes. The above results suggest that cyclohexanol induces the T → R transition in native insulin. Four semisynthetic insulin analogs, [Trp^{B25}]-, [Trp^{B26}]-, [Gly^{B24},Trp^{B25}]-, and [Gly^{B24},-Trp^{B26}]insulin, which all have a single tryptophan substitution in the C-terminal region of the B-chain, were prepared to assess changes in the environment of the substituted tryptophan residue during dimerization, hexamer formation, and the T → R transition using fluorescence spectroscopy. The absence of tryptophan in native insulin allowed the environment of the substituted residue to be analyzed specifically. The binding affinity of these analogs is displayed in Table 1. Since both phenol and cyclohexanol induce the T → R transition, the latter was used for these studies, because cyclohexanol does not interfere with the fluorescence emission of tryptophan. Figure 3 shows the fluorescence spectra of solutions of 4 μM analog alone or in the presence of 250 μM (1.45 mg/mL) native porcine insulin, in the presence and absence of Zn^{2+} and cyclohexanol. Native insulin is monomeric at 4 μM, but at 250 μM forms dimers, and forms hexamers in the presence of Zn^{2+} (Goldman & Carpenter, 1974). Changes in the fluorescence spectra of the analogs, upon the addition of a large excess of native insulin, indicate association of the analogs into insulin oligomers (i.e., dimers and hexamers) in which the analogs act as fluorescence probes.

Table 1: Relative Receptor Binding Potencies of Insulin and Insulin Analogs[a]

peptide/protein	relative potency (%)	peptide/protein	relative potency (%)
insulin	100	[Gly^{B24},Trp^{B25}]insulin	0.33
[Trp^{B25}]insulin	2.9	[Gly^{B24},Trp^{B26}]insulin	8.7
[Trp^{B26}]insulin	18		

[a] The analogs used in this study and their relative receptor binding potencies are identified above. Details of semisynthetic methods and of cell incubation procedures are provided under Materials and Methods. Relative receptor binding potency is defined as [(concentration of porcine insulin causing half-maximal inhibition of binding of [[^{125}I]iodo-Try^{A14}]insulin to receptor)/(concentration of analog causing half-maximal inhibition of binding of [[^{125}I]iodo-Try^{A14}]insulin to receptor] × 100. Each value represents the mean of 2–4 trials and displayed considerable consistency. The relative binding potencies reported in the table can be considered under most circumstances to reflect relative binding affinities.

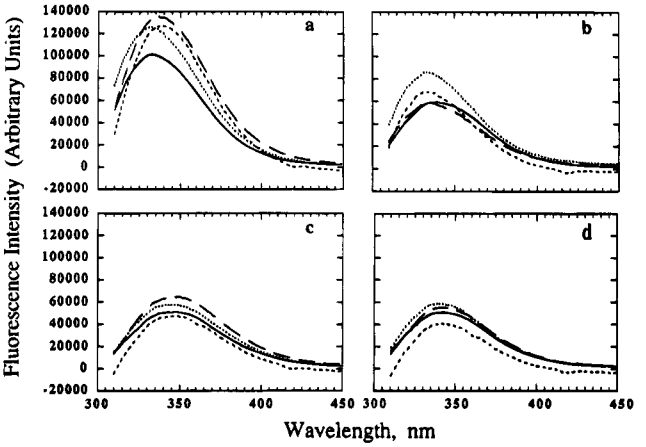

FIGURE 3: Fluorescence tracing of the association of tryptophan-substituted analogs with native insulin. Panels a–d illustrate the fluorescence emission spectra of (a) [Trp^{B25}]insulin, (b) [Trp^{B26}]-insulin, (c) [Gly^{B24},Trp^{B25}]insulin, and (d) [Gly^{B24},Trp^{B26}]insulin due to excitation at 295 nm. For each panel, 4 μM analog alone is represented by (—); 4 μM analog in the presence of 250 μM (1.45 mg/mL) native porcine insulin by (— —); analog + insulin + 0.08 mM $ZnSO_4$ by (- - -); and analog + insulin + Zn^{2+} + 360 mM cyclohexanol by (• • •). All solutions are in 0.1 M Tris/ClO_4^- buffer at pH 7.6, and background has been subtracted in all scans.

[Trp^{B25}]insulin. As shown in Figure 3a, the association of [Trp^{B25}]insulin with native insulin results in an increase in fluorescence intensity, which is possibly due to efficient energy transfer from nearby (≤14 Å) tyrosine residues (Weber, 1960), upon dimerization of the analog with native insulin. This increase in fluorescence intensity is accompanied by a 4 nm red shift in the emission maximum from 332 to 336 nm, suggesting movement of the tryptophan

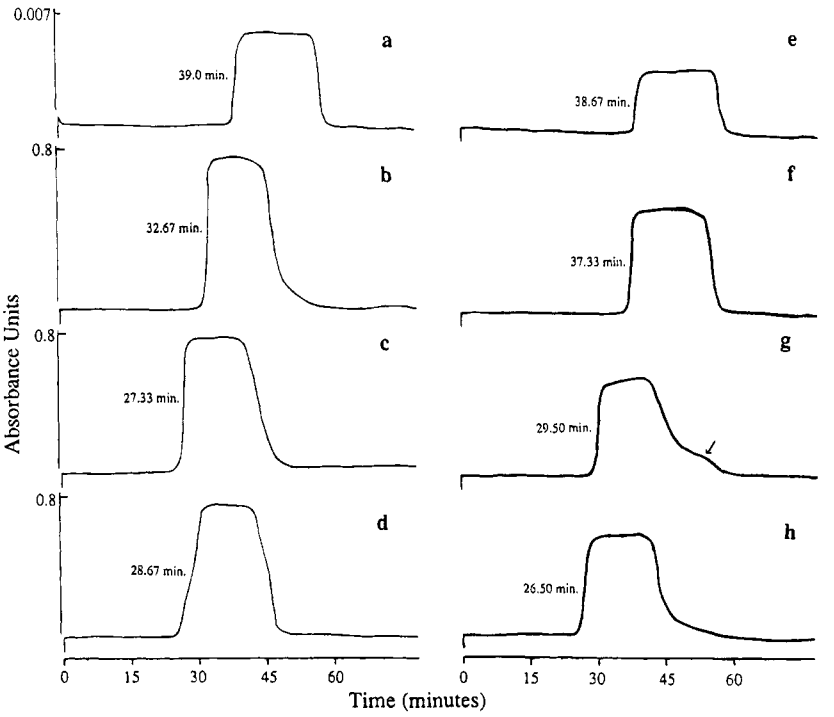

FIGURE 4: FPLC column elution studies to determine the aggregation state of native insulin (a–d) and DOI (e–h). In each case the FPLC column was preequilibrated for ≥12 h with the buffer solution desired in the absence of insulin. (a) Illustrates the elution time of 1 μM insulin in 0.1 M Tris/ClO_4^- buffer at pH 7.6; absorbance units full scale (AUFS) = 0.01, reading at 275 nm for tyrosine absorbance. (b) 200 μM insulin in buffer, (c) 200 μM insulin + 66.7 μM $ZnSO_4$ in buffer, and (d) 200 μM insulin + 66.7 μM $ZnSO_4$ + 360 mM cyclohexanol in buffer, detecting absorbance at 285 nm, AUFS = 1. (e) 1 μM DOI in buffer, absorbance detected at 275 nm and absorbance units full scale (AUFS) = 0.01. (f) 200 μM DOI in buffer, (g) 200 μM DOI + 66.7 μM $ZnSO_4$, and (h) 200 μM DOI + 66.7 μM $ZnSO_4$ + 360 mM cyclohexanol detected at 285 nm, AUFS = 1. The midpoint of the leading edge ($t_{e1/2}$) of each elution profile is given in minutes.

side chain to a more solvent-exposed environment (Lakowicz, 1983b). Upon the addition of Zn^{2+} to the solution of 4 μM analog + 250 μM native insulin, there is a further red shift to λ_{max} = 340 nm, suggesting further change in the environment of the tryptophan side chain. When cyclohexanol is added to the above solution, there is a blue shift of approximately 8 nm in the fluorescence emission maximum, consistent with the movement of the tryptophan to a more hydrophobic environment, possibly closer to the hydrophobic core of its respective insulin monomer, or closer to the dimer interface. In later experiments, we will present evidence that the tryptophan residue at position B25 of this analog moves toward the hydrophobic core of its respective monomer, assuming a molecule I-like orientation. These data suggest, however, that a change in conformation at one end of the insulin molecule, possibly the formation of the B-chain N-terminal helix of the R-state, has been accompanied by a structural change at the other end of the molecule (the B-chain carboxy-terminal position of the substituted tryptophan residue).

[Trp^{B26}]insulin. [Trp^{B26}]insulin also demonstrated fluorescence changes in the presence of excess native insulin, Zn^{2+}, and cyclohexanol, as illustrated in Figure 3b. The spectra of [Trp^{B26}]insulin differ, however, from those of [Trp^{B25}]insulin: when [Trp^{B26}]insulin associates with native insulin, the fluorescence spectra display a blue shift, indicating that the tryptophan residue has moved to a more hydrophobic environment. No additional spectral shifts occur when Zn^{2+} and cyclohexanol are added to this mixture, suggesting that neither hexamerization nor the T → R transition alters the environment of position B26.

[Gly^{B24},Trp^{B25}]insulin and [Gly^{B24},Trp^{B26}]insulin. The fluorescence spectra of [Gly^{B24},Trp^{B25}]insulin and [Gly^{B24},-Trp^{B26}]insulin are shown in Figure 3, panels c and d, respectively. These analogs show modest changes in fluorescence emission wavelength maxima and fluorescence intensity upon the addition of excess native insulin, Zn^{2+}, and cyclohexanol. We will show later that the analogs are, in fact, incorporated into hexameric complexes with native insulin. Nakagawa and Tager (1993) have previously shown that [Gly^{B24}]insulin forms hexamers; thus, the fluorescence spectra in Figure 3c,d suggest that these two analogs are incorporated into hexamers and may retain a conformation similar to the T-state of insulin.

State of Aggregation of Insulin and Insulin/Insulin Analog Mixtures. The data presented in the previous section suggested that [Trp^{B25}]-, [Trp^{B26}]-, [Gly^{B24},Trp^{B25}]-, and [Gly^{B24},Trp^{B26}]insulin associate with native insulin, possibly forming Zn^{2+}-coordinated hexamers and apparently undergoing the T → R transition. A gel filtration technique was used to assess the aggregation state of different solutions of insulin and insulin analogs, including *des*-octapeptide insulin (DOI) which cannot dimerize (Liang et al., 1985). As described in Materials and Methods, in this technique a large volume (6 mL) of a protein solution is injected onto a column (total volume = 24 mL). The state of aggregation is indicated by the position of the leading edge of the peak. Because of the large injection volume, the leading edge is followed by a plateau, the height of which reflects the concentration of the injected sample.

Figure 4a–d displays the FPLC elution patterns of solutions of insulin under various conditions; the midpoint

of the leading edge of each peak is given in minutes, and this time will be referred to as $t_{el/2}$. Figure 4a illustrates that 1 μM insulin, which is primarily monomeric (MW $\approx$ 5800) (Goldman & Carpenter, 1974), elutes from the FPLC column with $t_{el/2}$ = 39 min. The elution profile of 200 μM insulin, which is predominantly dimeric (Figure 4b), has a $t_{el/2}$ = 32.67 min, consistent with the molecular weight of the dimeric complexes (MW $\approx$ 11 600). Figure 4c illustrates the elution profile of 200 μM insulin in the presence of zinc-(II), i.e., predominantly hexameric insulin (Blundell et al., 1972); the $t_{el/2}$ = 27.33 min, consistent with MW $\approx$ 34 800. Figure 4d illustrates the elution spectra of 200 μM insulin in the presence of Zn^{2+} and cyclohexanol. Although, there is a slight shift to the right in the elution of this sample, the solution still appears to contain mostly hexamers, and $t_{el/2}$ = 28.67 min.

DOI was also studied using the same FPLC techniques previously described for native insulin (Figure 4e–h). Figures 4e,f demonstrates that 200 μM DOI, unlike native insulin, does not form dimers and accordingly elutes at the same relative position as 1 μM DOI and 1 μM insulin, which are both monomeric. However, in the presence of Zn^{2+} (Figure 4g) there is a distinct shift to the left in the elution profile, indicating that a higher molecular weight complex has been formed. The tail of this peak, however, trails through the monomeric region of the spectra (see arrow). As shown in Figure 4h, the addition of cyclohexanol eliminates this trailing edge in the chromatographic profile. These data indicate that DOI forms stable higher order aggregates in the presence of Zn^{2+}; the elution time of DOI in the presence of Zn^{2+} indicates an apparent MW $\approx$ 28 800, consistent with that of a DOI hexamer. Figure 4g,h shows the FPLC elution profiles of hexameric DOI, and hexameric DOI in the presence of cyclohexanol, respectively; Figure 4c,d shows the profiles of native insulin under the same conditions. The addition of cyclohexanol to hexameric DOI decreases the trailing (monomeric) portion of the peak, suggesting that DOI hexamers become more stable in the presence of cyclohexanol. In addition, there is a left shift of the ascending edge of the peak, perhaps indicating the presence of even higher oligomers, e.g., octamers.

Analysis of [Trp^{B26}]insulin and [Gly^{B24},Trp^{B26}]insulin Hexamer Formation. To further investigate the association of the tryptophan analogs with native insulin, two of the four insulin analogs were analyzed by the above FPLC column technique, and eluted fractions were collected. Initially, the state of aggregation of 50 μM native insulin (Figure 5a) was found to be identical to that of 200 μM insulin (Figure 4a–d), i.e., primarily dimeric in the absence of Zn^{2+} and hexameric in the presence of 66.7 μM Zn^{2+}. The elution profile of 50 μM insulin in the presence of 1 μM [Trp^{B26}]-insulin or [Gly^{B24},Trp^{B26}]insulin, as well as analog alone, were investigated; and fluorescence emission spectra of the fractions were measured to determine whether the tryptophan-substituted analogs would elute with native insulin under the chosen conditions (Figure 5). The FPLC elution profile of [Trp^{B26}]insulin, shown in Figure 5b, shows the elution position of 1 μM [Trp^{B26}]insulin determined via fluorescence analysis of the collected elution fractions. The elution time of 1 μM [Trp^{B26}]insulin was found to match that of 1 μM native insulin monomer (compare panels a and b, Figure 5). Figure 5b also displays a change in the elution position of [Trp^{B26}]insulin in the presence of 50 μM native

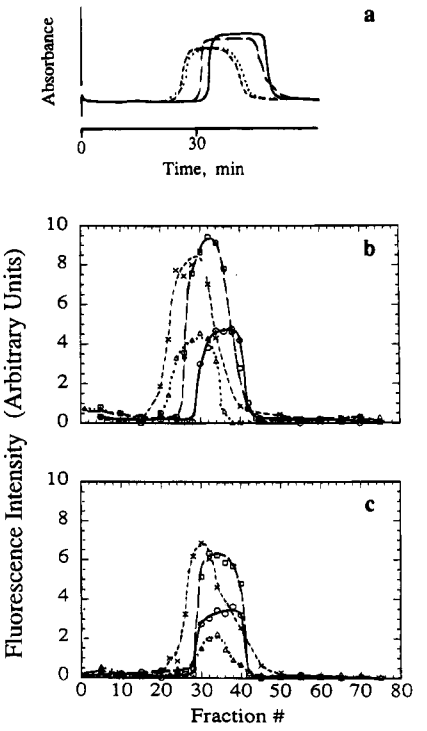

FIGURE 5: FPLC analysis of insulin and tryptophan-substituted insulin analogs. In all panels, (—) represents 1 μM analog; 1 μM analog + 50 μM insulin is represented by (– –); 1 μM analog + 50 μM insulin + 66.7 μM $ZnSO_4$ by (- - -); and the addition of 360 mM cyclohexanol to the previous mixture by (•••). Panel a illustrates the elution spectra of insulin, detecting absorbance at 275 nm for 1 μM insulin, and at 285 nm for the solutions of higher concentrations of insulin. Panels b and c are the elution profiles of [Trp^{B26}]insulin and [Gly^{B24},Trp^{B26}]insulin, respectively. Fractions were collected in 1.33 min intervals and measured via fluorescence emission at 335 nm, while exciting at 295 nm. All solutions are in 0.1 M Tris/ClO_4^- buffer at pH 7.6.

insulin, and in the presence of 50 μM native insulin and 66.7 μM Zn^{2+}. The analog elutes in earlier fractions in the presence of 50 μM insulin and is in the same position as 50 μM native insulin alone. Therefore, [Trp^{B26}]insulin forms dimers with native insulin. The addition of Zn^{2+} to a solution of 1 μM [Trp^{B26}]insulin plus 50 μM native insulin resulted in a shift of the peak to the left (Figure 5b), suggesting that [Trp^{B26}]insulin also forms stable hexamers with native insulin in the presence of Zn^{2+}. This shift in elution time was identical to that of 50 μM native insulin plus Zn^{2+}, in the absence of analog (compare panels a and b, Figure 5). The effect of cyclohexanol, which causes the T $\rightarrow$ R transition in native insulin, on the mixture was then investigated. A decrease in the fluorescence intensity was noted, although the elution position did not change.

Figure 5c illustrates the fluorescence elution profile of [Gly^{B24},Trp^{B26}]insulin. Hua et al. (1991) previously showed that Gly^{B24} analogs do not maintain the characteristic insulin fold. Thus, the [Gly^{B24},Trp^{B26}]insulin can be compared to the [Trp^{B26}]insulin since both analogs have tryptophan in the same position. Figure 5c shows that monomeric [Gly^{B24},-Trp^{B26}]insulin elutes in the same position as monomeric native insulin, just as [Trp^{B26}]insulin did; however, upon combination of 1 μM [Gly^{B24},Trp^{B26}]insulin with 50 μM native insulin, the analog still elutes at the monomeric position. This result indicates that, unlike [Trp^{B26}]insulin, [Gly^{B24},Trp^{B26}]insulin does not codimerize with native insulin. The inability of [Gly^{B24},Trp^{B26}]insulin to form such

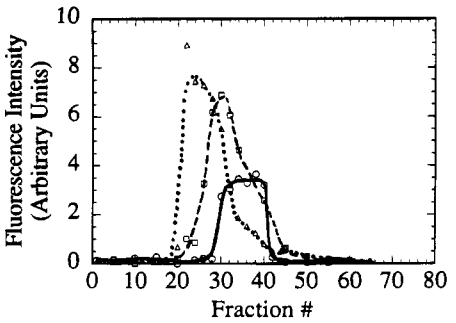

FIGURE 6: FPLC elution profile of [Gly^{B24},Trp^{B26}]insulin in 0.1 M Tris/ClO_4^- buffer at pH 7.6 at 1 μM (—); 1 μM [Gly^{B24},Trp^{B26}]-insulin + 50 μM insulin + 66.7 μM $ZnSO_4$ (- - -); 1 μM [Gly^{B24},-Trp^{B26}]insulin + 50 μM DOI + 66.7 μM $ZnSO_4$ (• • •). Fractions were collected in 1.33 min intervals, and the fluorescence emission was measured at 335 nm, while exciting at 295 nm.

codimers may be due to the lack of a defined β-sheet region in this analog. Upon the addition of 66.7 μM Zn^{2+} to the solution of 1 μM [Gly^{B24},Trp^{B26}]insulin and 50 μM native insulin, as described previously, the analog elutes in earlier fractions, suggesting that [Gly^{B24},Trp^{B26}]insulin aggregates with native insulin in the presence of Zn^{2+}. The elution position of these higher molecular weight aggregates suggests that they are mixed hexamers of [Gly^{B24},Trp^{B26}]insulin and native insulin. These hexameric complexes, however, appear less stable than the mixed hexamers of native insulin and [Trp^{B26}]insulin mentioned earlier, as shown by the prominence of less highly aggregated species (dimers and monomers) in the elution profile of [Gly^{B24},Trp^{B26}]insulin hexamers. Furthermore, the addition of cyclohexanol causes the fluorescence elution spectrum of the Zn^{2+}-coordinated hexamers of [Gly^{B24},Trp^{B26}]insulin to shift back to a monomeric position (Figure 5c). It is probable that native insulin undergoes the T → R transition and thereby destabilizes the [Gly^{B24},Trp^{B26}]insulin mixed hexamer, causing the analog to be excluded from the insulin hexamers.

The ability of [Gly^{B24},Trp^{B26}]insulin to form mixed hexamers with DOI was also investigated via fluorescence analysis of FPLC elution fractions. Figure 6 illustrates the elution profile of [Gly^{B24},Trp^{B26}]insulin in mixed hexamers with native insulin or DOI, both in the presence of Zn^{2+}. [Gly^{B24},Trp^{B26}]insulin appears to form hexameric complexes with DOI, indicated by the earlier elution time of the analog when in association with Zn^{2+}-coordinated DOI. This contrasts with the profile of 1 μM [Gly^{B24},Trp^{B26}]insulin + 50 μM insulin + Zn^{2+} in which dimers and monomers predominate the fluorescence profile. Thus, the absence of the β-sheet region in DOI may allow the formation of stable mixed hexamers with [Gly^{B24},Trp^{B26}]insulin, whereas mixed hexamers are destabilized by native insulin.

Conformational Adjustments in Monomeric Insulin. Hexameric complexes of native insulin are believed to have binding pockets, consisting of two dimers of the hexamer, for specific cyclic alcohols, such as, phenol, *m*-cresol, and cyclohexanol (Derewenda et al., 1989; Brader et al., 1991). The results from the CD studies described previously, particularly the studies utilizing 3-pentanol to induce the T → R transition, raised the following questions: (a) how specific is the binding pocket for alcohol ligands? and (b) does this pocket exclusively exist between dimers of a coordinated hexamer, or is it a property of each monomer in an (R_6) insulin hexamer?

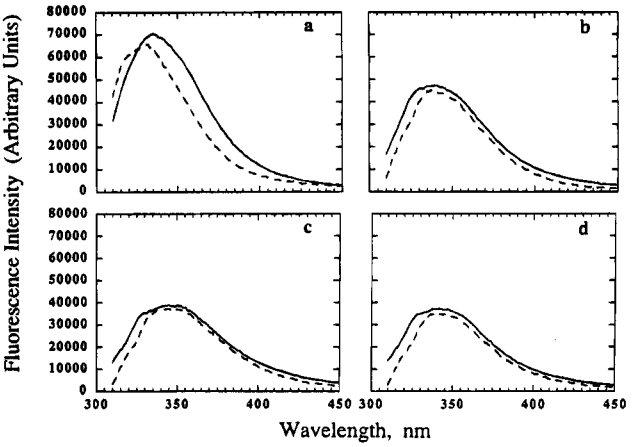

FIGURE 7: Fluorescence analysis of monomeric tryptophan-substituted analogs. Panels a–d illustrate the fluorescence emission spectra of (a) [Trp^{B25}]insulin, (b) [Trp^{B26}]insulin, (c) [Gly^{B24},Trp^{B25}]-insulin, and (d) [Gly^{B24},Trp^{B26}]insulin at a concentration of 2 μM in the absence (—) and presence (- - -) of 360 mM cyclohexanol. All of the solutions are in 0.1 M Tris/ClO_4^- buffer at pH 7.6 and were excited at 295 nm for tryptophan fluorescence.

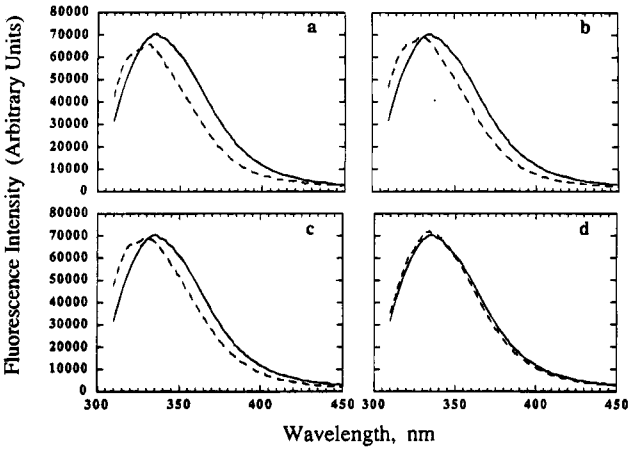

FIGURE 8: Fluorescence emission spectra of [Trp^{B25}]insulin. The analog is at a primarily monomeric concentration of 2 μM in 0.1 M Tris/ClO_4^- buffer at pH 7.6. The fluorescence emission spectra are represented in each panel in the absence (—) and presence (- - -) of a specific alcohol ligand: (a) cyclohexanol, (b) 3-pentanol, (c) cyclopentanol, and (d) 2-propanol, all at 360 mM. Each spectrum is the result of excitation at 295 nm as described in Materials and Methods.

Figure 7 displays the fluorescence spectra of [Trp^{B25}]-, [Trp^{B26}]-, [Gly^{B24},Trp^{B25}]-, and [Gly^{B24},Trp^{B26}]insulin analogs at 2 μM concentrations. The addition of Zn^{2+} or Co^{2+} had no effect on the fluorescence spectra, suggesting that these four semisynthetic analogs, like native insulin (Goldman & Carpenter, 1974), are monomeric at 2 μM concentration. The addition of cyclohexanol, however, causes a blue shift of approximately 7 nm (from 335 to 328 nm) in the fluorescence emission maximum of [Trp^{B25}]insulin (Figure 7a), suggesting that the alcohol ligand causes the tryptophan at position B25 to move to a more hydrophobic environment, perhaps closer to the core of the insulin monomer.

The specificity of the conformational change in monomeric [Trp^{B25}]insulin due to the binding of cyclohexanol was investigated by comparing the effects of cyclohexanol, 3-pentanol, cyclopentanol, and 2-propanol. As shown in Figure 8a–d, cyclopentanol and 3-pentanol also cause a blue shift in the fluorescence spectrum of a 2 μM solution of [Trp^{B25}]insulin; at this concentration, native insulin is mon-

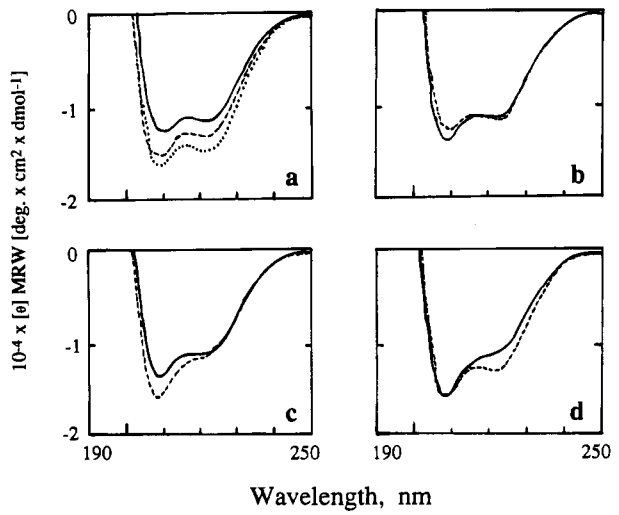

FIGURE 9: Circular dichroic spectra of native insulin. Panel a illustrates the CD spectra of insulin plus 0.17 mM $ZnSO_4$ in 0.1 M Tris/ClO_4^- buffer at pH 7.6 (—), plus 360 mM cyclohexanol (- - -), and plus 360 mM cyclohexanol and 250 mM NaCl (• • •). Panel b illustrates insulin in buffer (—), and in the presence of 0.17 mM $ZnSO_4$ (- - -). Panel c shows insulin (—) and insulin in the presence of cyclohexanol (- - -). Panel d compares the effects of 360 mM cyclohexanol on native insulin in the absence (—) and presence (- - -) of 0.17 mM $ZnSO_4$. Insulin is at 2.9 mg/mL in each spectra, and all solutions are in 0.1 M Tris/ClO_4^- buffer at pH 7.6.

omeric. In contrast to the other alcohols, 2-propanol did not cause the characteristic blue shift, nor any other change in the fluorescence spectrum of [Trp^{B25}]insulin. The other analogs displayed essentially no change in their fluorescence spectra under the same conditions (data not shown). Both the occurrence of a blue shift in the fluorescence spectrum of [Trp^{B25}]insulin, caused by alcohol ligands, and the order of effectiveness of these ligands (cyclohexanol ≈ 3-pentanol ≈ cyclopentanol ≫ 2-propanol) are reminiscent of the T → R transition in hexameric complexes mentioned earlier. If this proposition were correct, then the monomeric form of [Trp^{B25}]insulin would have undergone a conformational change similar to the T → R transition, previously observed only in insulin hexamers.

Circular dichroic studies were then undertaken to determine if native insulin could be induced to undergo a change in secondary structure, due to the binding of an alcohol ligand, in the monomeric and dimeric state, i.e., as opposed to the hexameric state. Figure 9a shows the circular dichroic changes that accompany a typical T → R transition in Zn^{2+}-coordinated hexameric insulin. The increase in negative ellipticity when cyclohexanol is added to the hexameric complexes is consistent with the formation of an extra α-helical region (R-state) (Wollmer et al., 1987), which is then further stabilized by the addition of monovalent anions, such as, SCN^- and Cl^- (Wollmer et al., 1989). Figure 9b compares Zn^{2+}-free insulin to hexameric insulin formed when Zn^{2+} is added to the solution. Upon the addition of Zn^{2+}, there is a decrease in the negative ellipticity at 208 nm and a slight increase at 222 nm. These spectra show that the structure of hexameric T-state insulin (Blundell et al., 1972; Baker et al., 1988) is not identical to that of Zn^{2+}-free (dimeric/monomeric) T-state insulin. The slight increase in negative ellipticity at 222 nm, with a concomitant decrease at 208 nm, in Figure 9b, suggests the stabilization of β-sheet structure as hexamer formation occurs. In contrast, *des*-octapeptide(B23−30)insulin (DOI), which cannot dimerize because it lacks the putative dimerization site, but forms hexamers in the presence of Zn^{2+}, had identical CD spectra in the absence or presence of Zn^{2+} (data not shown). Thus, the change in the CD spectra of native insulin may be due to alterations in the carboxy-terminal β-sheet region of the B-chain—i.e., the segment missing from DOI, which does not show this spectral change. The larger decrease in negative ellipticity at 208 nm also suggests that hexameric insulin may, in fact, have slightly less helical content than nonhexameric insulin in solution. A comparison of the crystal structure of dimeric insulin versus 2-Zn insulin hexamers illustrates an apparent difference in the orientation of the N-terminal B-chain residues [cf. Derewenda et al. (1990)]. The N-terminus of dimeric insulin is less restricted and displays a greater degree of conformational freedom than in the T-state hexamer.

The above data suggest that two similar but nonidentical T-state conformations can be identified: (1) T_M, the metal coordinated conformation of hexameric insulin (Blundell et al., 1972; Baker et al., 1988), and (2) T_I, which exists independent of metal ion coordination, as shown in Figure 9b. In an attempt to determine if alcohol ligands could cause native insulin to undergo a conformational change in the absence of hexamer formation, CD spectra were taken of insulin in the presence, and absence, of cyclohexanol. Figure 9c demonstrates that cyclohexanol causes a pronounced increase in negative ellipticity in the 208-nm region ($-[\theta]_{208}$) of the CD spectrum of Zn^{2+}-free insulin in solution, but without a concomitant increase in $-[\theta]_{222}$. This suggests the formation of additional α-helices in the insulin molecules due to the binding of cyclohexanol; however, unlike the classical T → R transition of hexameric complexes, nonhexameric insulin displays a distinct increase in the $[\theta]_{208}/[\theta]_{222}$ ratio. Figure 9d shows that cyclohexanol increases the negative ellipticity at 208 nm of both hexameric, Zn^{2+}-coordinated insulin, or Zn^{2+}-free insulin to the same extent. In contrast, there is an increase in $-[\theta]_{222}$ with the addition of Zn^{2+}. These data suggest that the binding of cyclohexanol to dimeric, Zn^{2+}-free insulin results in the formation of additional α-helix. It is also highly likely that the additional α-helical region is at the N-terminus of the B-chain. Thus, in the presence of cyclohexanol, dimeric insulin appears to adopt a conformation similar, but not identical to the classical R-state of Zn^{2+}-coordinated hexameric insulin. The term R_I will be used for the conformation of Zn^{2+}-free insulin in the presence of cyclohexanol, because it forms a structure similar to metal coordinated R-state insulin (R_M) in a metal ion-independent manner.

The CD spectra of hexameric and nonhexameric insulin, in the presence of cyclohexanol, differ at 222 nm, but not at 208 nm; i.e., they differ in the region of the spectrum defined by β-sheet, as well as α-helix. This spectral difference might be explained by the presence of a stable β-sheet structure in Zn^{2+}-coordinated hexameric insulin—a β-sheet structure which may be absent or distorted in Zn^{2+}-free insulin in the presence of cyclohexanol. Since the β-sheet is also the putative dimerization site, it is possible that loss or distortion of this structure could be the result of dissociation of the dimers. This possibility was investigated by comparing the FPLC elution profile of insulin, and insulin in the presence

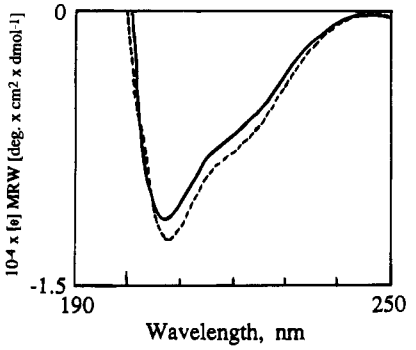

FIGURE 10: CD spectra of 2.4 mg/mL DOI in the absence (—) and presence (- - -) of 360 mM cyclohexanol. Both solutions are in 0.1 M Tris/ClO_4^- buffer at pH 7.6.

of cyclohexanol. It was found that the FPLC peaks of insulin in the presence, and absence, of cyclohexanol had essentially superimposable leading edges, indicating that cyclohexanol does not cause insulin dimers to dissociate to monomers under these experimental conditions (data not shown). These results suggest that in the R_I-state the β-sheet is altered without causing dissociation of the dimeric complexes.

The distortion of β-sheet structure is further elucidated by the analysis of *des*-octapeptide insulin (DOI), which lacks the β-sheet segment, in the absence, and presence, of the alcohol ligand cyclohexanol (Figure 10). The addition of cyclohexanol to DOI increases both $-[\theta]_{208}$ and $-[\theta]_{222}$. In this respect, the CD spectra of DOI resemble that of Zn^{2+}-coordinated insulin, but differs from that of Zn^{2+}-free insulin (Figure 9c). Thus, both the 208- and 222-nm regions of the CD spectra describe an increase in the α-helical content of DOI. These results suggest that, in the R_I-state, cyclohexanol alters nonhexameric insulin at the COOH-terminus of the B-chain, resulting in the distortion or loss of β-sheet structure. This carboxy-terminal region is absent in DOI; therefore, the changes in β-sheet structure are absent in DOI, and only changes in α-helix are observed. In other words, the R_I-state is similar in α-helical content to the hexameric R_M-state; however, in the R_M-state, but not in the R_I-state, the β-sheet region is stabilized by hexameric coordination. Subsequently, when the R_I-state is induced, the increase in negative ellipticity from 215 to 222 nm, due to α-helix formation, is disguised by the simultaneous decrease in β-sheet content, which is detected within the same spectral range.

The above CD results suggest the following: (a) Conformational changes in one region of native insulin, notably the induction of α-helix at the B-chain N-terminus, cause distant global changes in structure at the carboxy-terminal β-strand region of the molecule. The crystal structures of T_3R_3 and R_6 insulin hexamers support this hypothesis, demonstrating the separation of the COOH-terminal B-chain residues from the central B-chain helix in the R-state (Smith & Dodson, 1992; Ciszak & Smith, 1994). This implies that the changes seen in the fluorescence spectra of the tryptophan-substituted analogs, in the presence of specific alcohol ligands, are attributable to the formation of the extra α-helical R_I-state. (b) The ability of DOI to undergo a cyclohexanol-induced conformational change is consistent with the localization of the additional α-helices to the N-terminus of the B-chain, which are also present in hexameric insulin (R_M-state) (Chothia et al., 1983; Derewenda et al., 1989). (c)

Table 2: Comparison of Molecular Ellipticities of Insulin Due to Ligand Binding[a]

	θ_{208nm} (deg)	θ_{222nm} (deg)	$\theta_{208}/\theta_{222}$
insulin + cyclohexanol	−15 877	−11 379	1.40
insulin + cyclopentanol	−14 206	−11 068	1.28
insulin + 3-pentanol	−13 712	−11 071	1.24
insulin + 2-propanol	−13 901	−11 116	1.25
insulin (alone in buffer)	−13 770	−11 326	1.22

[a] The circular dichroic ellipticities of the observed Zn^{2+}-free solutions of insulin in the presence, and absence, of alcohol ligand are listed above. In each case, 2.9 mg/mL porcine insulin is in 0.1 M Tris/ClO_4^- buffer at pH 7.6. The specific alcohol ligand is at 360 mM concentration in each case, and background effects have been subtracted. All ellipticities are based on mean residual weight (MRW), with CD spectra taken as described in Materials and Methods.

The similar CD spectra of DOI, which cannot form dimers, and native insulin indicate that monomeric insulin can form a structure resembling the R-state.

The other alcohol ligands were also tested to assess their ability to induce the R_I-state. Table 2 lists the ellipticity of insulin at 208 and 222 nm, and the $[\theta]_{208}/[\theta]_{222}$ ratio, in the presence of the different alcohol ligands and alone in solution. In promoting the R_I-state, cyclohexanol ≫ cyclopentanol ≈ 3-pentanol ≈ 2-propanol. These results indicate that the alcohol specificity is actually higher for Zn^{2+}-free insulin in solution than it is for hexameric complexes, which displayed similar binding affinities for cyclohexanol, cyclopentanol, and 3-pentanol. Therefore, hexamer formation appears to assist the $T_M \rightarrow R_M$ transition by stabilizing otherwise unfavorable contacts of imperfect alcohol ligands binding to Zn^{2+}-free insulin. These results indicate that the binding of specific alcohol ligands by insulin is not due to a pocket formed by adjacent dimers of a hexamer, but is a property of individual insulin molecules in a monomeric or hexameric environment, in solution or in a crystal lattice.

Positional Adjustments of B25 and B26. Acrylamide was used as a fluorescence quenching agent to assess the solvent accessibility of the substituted tryptophan in the different analogs. Figure 11 illustrates the Stern−Volmer plots of tryptophan fluorescence quenching for each of the insulin analogs in the presence or absence of cyclohexanol, and the effects of cyclohexanol on the quenching of *N*-acetyltryptophan ethyl ester (NAWEE), a fully exposed tryptophan derivative. Table 3 gives the values for both the dynamic (K_{sv}, linear) and static (V, exponential) quenching constants as modeled using the modified Stern−Volmer equation (Eftink & Ghiron, 1976). The dynamic, or collisional, quenching constant, K_{sv}, results from collision of the fluorophore with a quencher in solution, followed by energy transfer to the quencher. The static quenching constant, V, is a measure of fluorescence quenching that occurs when a quenching molecule is so close to the fluorophore that energy transfer is essentially instantaneous. Both static and dynamic quenching requires the quenching molecule to come within a minimum radius of effective energy transfer, known as the "sphere of action". However, at higher concentrations of quencher, the probability approaches unity that there is a quencher within this distance, and static quenching is observed.

Figure 11a and Table 3 illustrate that [Trp^{B25}]insulin shows only dynamic quenching by acrylamide, as indicated by a straight line in the Stern−Volmer plot. The presence of

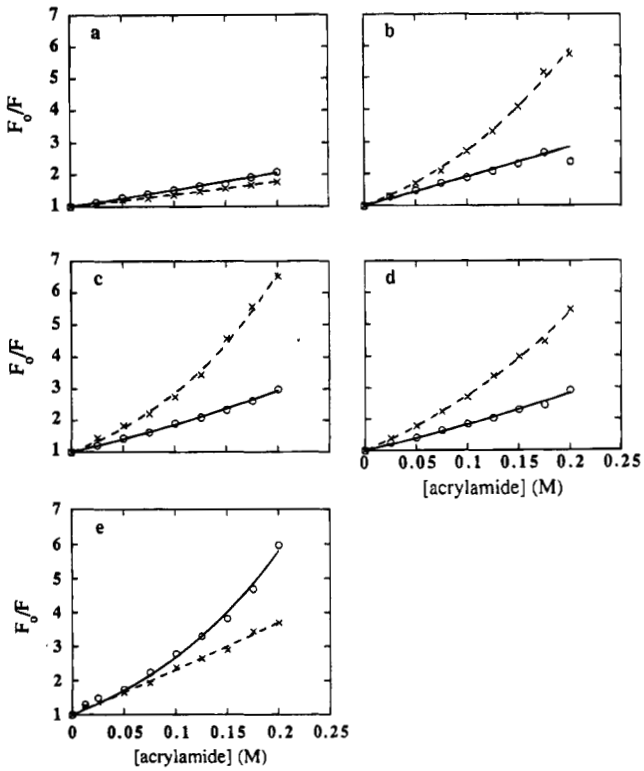

FIGURE 11: Acrylamide quenching of tryptophan fluorescence. Panels a–e illustrate the Stern–Volmer plots of 2 μM (a) [Trp^{B25}]-insulin, (b) [Trp^{B26}]insulin, (c) [Gly^{B24},Trp^{B25}]insulin, (d) [Gly^{B24},-Trp^{B26}]insulin, and (e) NAWEE in the absence (—) and presence (- - -) of 360 mM cyclohexanol. All solutions are in 0.1 M Tris/ClO_4^- buffer at pH 7.6 and are plotted as acrylamide concentration, [Q] (0–200 mM), versus F_0/F (degree of fluorescence quenching) modeled via the modified Stern–Volmer equation $F_0/F = (1 + K_{SV}[Q])e^{V[Q]}$; where F_0 is the tryptophan fluorescence emission in the absence of quenching agent, F is the fluorescence at a given acrylamide concentration, K_{SV} is the Stern–Volmer dynamic quenching constant, and V is the static quenching constant. Note, from the equation above, that in the limit of $V \rightarrow 0$, the equation describes a linear function $F_0/F = (1 + K_{SV}[Q])$, in which the degree of quenching is totally defined by K_{SV}, the dynamic (collisional) quenching constant. All measurements were taken at the fluorescence emission maximum for the solution being analyzed, which is listed in Table 2.

cyclohexanol causes a slight decrease in the dynamic quenching constant, displayed as a decrease in the slope of the Stern–Volmer plot, indicating the movement of the tryptophan to a less solvent-exposed position. This result is consistent with the blue shift in the fluorescence emission spectrum of this analog. The other analogs (Figure 11b–d) show a higher dynamic quenching constant than [Trp^{B25}]-insulin, suggesting that, in these analogs, the tryptophan is more solvent exposed than in [Trp^{B25}]insulin. Moreover, the addition of cyclohexanol to [Trp^{B26}]-, [Gly^{B24},Trp^{B25}]-, and [Gly^{B24},Trp^{B26}]insulin analogs induces a significant static quenching component not observed for [Trp^{B25}]insulin, nor in the other analogs in the absence of cyclohexanol. This static quenching, which causes the Stern–Volmer plot to become curved, suggests that cyclohexanol induces a conformational change, allowing for even greater solvent exposure of the substituted tryptophan than occurs in the absence of cyclohexanol. In other words, the tryptophan in [Trp^{B26}]-, [Gly^{B24},Trp^{B25}]-, and [Gly^{B24},Trp^{B26}]insulin is moved to a new environment in which the "effective" concentration of acrylamide is higher, as a result of the cyclohexanol-induced conformational change. The results for [Trp^{B26}]insulin indicate a subtle conformational change induced by cyclohexanol which did not affect the fluorescence emission spectrum shown in Figure 7b. These results also show that the tryptophan in the glycine-containing analogs (Figure 11c,d) is more solvent exposed than that of [Trp^{B25}]- and [Trp^{B26}]insulin, displaying higher static quenching constant values in Table 3 and a red-shifted emission maximum of 345 nm.

The effects of cyclohexanol on these analogs can be compared to its effect on the acrylamide-induced quenching of NAWEE, a solvent-exposed tryptophan derivative (Figure 11e). In buffer (no cyclohexanol), acrylamide quenching has a large dynamic quenching coefficient, consistent with free access of quencher to the solvent-exposed fluorophore. In addition, there is a large static component to the quenching, which can be attributed to the high probability of an acrylamide molecule being within the appropriate distance for instantaneous energy transfer at high acrylamide concentrations (Lakowicz, 1983c). The addition of cyclohexanol eliminates the static component, perhaps because cyclohexanol reduces the probability of an acrylamide molecule being within the quenching sphere of action by lowering the "effective" concentration of acrylamide surrounding a NAWEE molecule. In any case, the effect of cyclohexanol on NAWEE is opposite to its effect on the insulin analogs. Thus, the effect of cyclohexanol on the fluorescence quenching of the analogs cannot be ascribed solely to the effects of cyclohexanol on solvent structure. Rather, these results indicate that cyclohexanol induces a conformational change in the insulin analogs.

DISCUSSION

T → R Transition in Hexameric Insulin. The work presented in this paper demonstrates that the induction of the T → R transition in metal-coordinated insulin by several alcohol ligands, including cyclohexanol, is not always reflected by changes in the visible absorbance spectrum. Phenol, cyclohexanol, and 3-pentanol all increase the absorbance spectrum of a solution of insulin$_6$(Co^{2+})$_2$ which has been previously associated with the $T_6 \rightarrow R_6$ conformational transition (Roy et al., 1989; Thomas & Wollmer, 1989; Nakagawa & Tager, 1991). Cyclopentanol and 2-propanol do not induce these absorbance changes, however, despite the fact that circular dichroic spectroscopy shows that these alcohols induce the formation of an extra α-helical region (characteristic of the R-state) in Zn^{2+}-coordinated hexamers. In fact, cyclopentanol causes an increase in negative ellipticity on the CD spectra to a degree almost indistinguishable from that of cyclohexanol or 3-pentanol. Phenol could not be tested because of the intense absorbance of phenol.

Tryptophan-containing insulin analogs ([Trp^{B25}]-, [Trp^{B26}]-, [Gly^{B24},Trp^{B25}]-, and [Gly^{B24},Trp^{B26}]insulin) were used as fluorescence probes of structural adjustments of insulin upon dimer and hexamer formation (Figure 3). These studies demonstrated that the environment of the tryptophan side chain at positions B25 and B26 changes upon dimer and mixed-hexamer formation with native insulin, a feature which may also be characteristic of native insulin as demonstrated by the alternate conformations of the COOH-terminus found in different crystal structures. Spectral changes were also

Table 3: Fluorescence Quenching Constants for Stern−Volmer Plots[a]

protein: tryptophan fluorescence source	solvent	wavelength of emission max, nm	dynamic quenching constant (K_{SV}), M^{-1}	static quenching constant (V), M^{-1}
[Trp^{B25}]insulin	buffer	335	4.99 ± 0.81	0.13 ± 0.45
	cyclohexanol	325	3.38 ± 0.55	0.29 ± 0.36
[Trp^{B26}]insulin	buffer	335	9.03 ± 1.20	0.50 ± 0.52
	cyclohexanol	335	8.50 ± 1.42	3.90 ± 0.58
[Gly^{B24},Trp^{B25}]insulin	buffer	345	6.64 ± 0.67	1.18 ± 0.32
	cyclohexanol	345	7.95 ± 1.40	4.69 ± 0.59
[Gly^{B24},Trp^{B26}]insulin	buffer	345	6.53 ± 1.12	1.02 ± 0.54
	cyclohexanol	345	11.5 ± 0.99	2.45 ± 0.34
NAWEE	buffer	345	7.97 ± 1.71	4.03 ± 0.72
	cyclohexanol	345	12.6 ± 1.12	0.28 ± 0.37

[a] The dynamic (K_{SV}), and static (V), quenching constants (with standard deviation) for each of the insulin analogs studied via acrylamide quenching. The constants represent the graphs in Figure 5, modeled by the modified Stern−Volmer equation: $F_0/F = (1 + K_{SV}[Q])e^{V[Q]}$ (Eftink & Ghiron, 1976), where F_0/F is the degree of fluorescence quenching, K_{SV} is the Stern−Volmer dynamic quenching constant, and V is the static quenching constant. In all cases the buffering solution used is 0.1 M Tris/ClO_4^- buffer at pH 7.6 and cyclohexanol is at 360 mM when present. All analogs, and NAWEE (*N*-acetyltryptophan ethyl ester), are at 2 μM. All values for the degree of fluorescence quenching, therefore the Stern−Volmer plots in Figure 11, as well as quenching constants, were obtained at the emission maximum of the particular fluorophore in the absence, and presence, of cyclohexanol.

noted when the T → R transition was induced with the alcohol ligand cyclohexanol. The changes in the fluorescence spectra of the mixed-hexameric complexes of native insulin and the tryptophan-substituted insulin analogs when the T → R transition occurs demonstrate that α-helix formation, at the N-terminus of the B-chain, causes a concomitant structural change at the C-terminus. These studies suggest that, in T-state insulin, Phe^{B25} is in a more solvent-exposed (molecule II-type) position which changes to a less solvent-exposed (molecule I-type) position upon assuming the R-state as inferred from the fluorescence spectra of [Trp^{B25}]insulin. [Gly^{B24}]insulin analogs can also be incorporated into a hexameric complex, which changes conformation after the addition of cyclohexanol. These hexamers, however, are apparently less stable than those of native insulin.

Oligomerization of insulin and insulin analogs was analyzed by an FPLC column technique (Figures 4−6). Using this technique, it was shown that DOI can form high molecular weight aggregates, including hexamers, in the presence of Zn^{2+} (Figure 4e−h) possibly via coordination with His^{B5} as in 4-Zn insulin (Chothia et al., 1983). The FPLC elution profile of DOI also suggests that the Zn^{2+}-coordinated DOI complexes are stabilized by the addition of cyclohexanol, possibly associated with the attainment of an R-like state. This stabilization of DOI may be due to the lack of the B-chain carboxy-terminus which, in native insulin, changes conformation upon assuming the R-state (Smith & Dodson, 1992; Ciszak & Smith, 1994).

Nonhexameric Conformational Adjustments (Monomeric/Dimeric). These studies suggest that, upon binding an alcohol ligand, monomeric insulin can be induced to undergo alterations in secondary structure. Circular dichroic studies of native insulin indicate that the structure of insulin in solution, in the absence of hexameric metal ion coordination, is not identical to the previously defined T_M-state (M: metal ion coordinated). Furthermore, these studies suggest that Zn^{2+}-free insulin in solution, in the T_I-state (I: independent of metal ion coordination), has less β-sheet structure, and possibly, a slightly higher degree of α-helical content, than metal-coordinated insulin hexamers in the T_M-state. It has previously been suggested by Wollmer that ≈2−5% of insulin in solution is probably in the R-state (personal communication). An alternate conformation of Zn^{2+}-free insulin has also been identified, called the R_I-state. This alternate conformation of insulin, which is induced by the binding of cyclohexanol, has a higher helical content than native insulin in solution. This newly formed α-helical region is most likely at the N-terminus of the B-chain. It should also be mentioned that the R_I-state is converted to the previously described R_M-state upon Zn^{2+}-coordinated hexamer formation.

CD studies were used to demonstrate that DOI could also assume a conformation similar to the R_I-state of native insulin, suggesting the following: (a) The R_I-state is a property of monomeric as well as dimeric insulin, since DOI cannot form dimers, yet displays a characteristic increase in α-helix in the presence of cyclohexanol like that of native insulin. (b) The absence of changes in ellipticity at 215−222 nm in native insulin, when the R_I-state is induced, is attributable to the loss or distortion of β-strand structure in the B-chain C-terminal residues. (c) When insulin in solution becomes metal ion coordinated, forming hexamers, the β-sheet is stabilized; subsequently, upon the addition of cyclohexanol to induce the $T_M \rightarrow R_M$ transition, this situation is maintained. This stabilization of β-sheet structure does not occur in the absence of hexamer formation, during the $T_I \rightarrow R_I$ conformational transition.

The concomitant conformational changes at the B-chain amino- and carboxy-terminus, in monomeric insulin, were further confirmed by fluorescence studies of insulin analogs. The fluorescence spectrum of a monomeric solution of [Trp^{B25}]insulin displays a blue shift in the presence of cyclohexanol. This spectral change indicates that the tryptophan side chain at position B25 of the C-terminal region has moved to a more hydrophobic environment. The formation of an extra α-helical region at the N-terminus of the B-chain of Zn^{2+}-free insulin (R_I-state) and the change in position of the tryptophan in [Trp^{B25}]insulin appear to be linked. Accordingly, the CD spectra of [Trp^{B25}]insulin in the presence of cyclohexanol displayed an increase in negative ellipticity at 208 nm (data not shown) much like that of native insulin (Figure 9c), suggesting that this analog does, in fact, assume the R_I-state. A similar conformational change was noted in the hexameric studies in which the T → R transition caused a blue shift in the fluorescence

FIGURE 12: Model of the different conformational states of metal-coordinated (hexameric), and monomeric, insulin. The thick line represents the B-chain, the thinner line represents the A-chain of an insulin monomer, and the amino-terminus of each chain is indicated by a ball. The arrow in each illustration gives the location of Phe^{B25}; phenol (or cyclohexanol) is represented as a striped hexagon; and hydrogen bonds are represented as dotted lines. It can be seen that the major difference between the metal-coordinated T_M- and R_M-states is the reorganization of hydrogen bonding at the B-chain N-terminus, allowing two additional turns of helix, and alteration of Phe^{B25} in the R_M-state. The T_I- and R_I-states, which are independent of metal ion coordination, differ in a similar manner; however, the β-sheet region of the B-chain carboxy terminus in the R_I-state is not as well-defined as in the R_M-state, as explained in the text. Accordingly, both the $T_M \rightarrow R_M$ hexameric transition and the $T_I \rightarrow R_I$ monomeric transition cause the amino acid side chain at position B25 to move to a more hydrophobic environment; however, position B25 is more solvent exposed in the T_M-state (molecule II-type) than in the T_I-state. The amino-terminus of the B-chain in the monomeric T_I-state is also depicted as having the conformational flexibility to twist and turn, unlike the hexameric T_M-state.

spectrum of $[Trp^{B25}]$insulin in Zn^{2+}-coordinated hexamers. These results suggest that the $T_I \rightarrow R_I$ transition causes the tryptophan side chain in the monomeric insulin analog to move from a previously more solvent-exposed (molecule II-like) position to a molecule 1-like position, using the Chinese nomenclature (Blundell et al., 1972).

The fluorescence quenching studies indicated that the tryptophan residue at position B25 is less solvent exposed than at position B26; and the tryptophan residues in the Gly analogs are the most solvent exposed. The quenching studies also suggested that $[Trp^{B26}]$insulin changes orientation when the R_I-state is induced, supporting the CD studies which indicated that the entire carboxy-terminus of the B-chain changes conformation when forming the R_I-state. The tryptophan at position B26 appears to move to a more solvent-accessible environment when the R_I-state is induced, unlike the tryptophan at position B25, which moves to a less solvent-exposed environment. Therefore, our data indicate that both positions B25 and B26 are altered in the $T_I \rightarrow R_I$ transition of monomeric insulin, but in a different manner.

A Defined Conformational Change in Monomeric Insulin. Figure 12 illustrates a model for the interaction of cyclohexanol with an insulin monomer. In the T_M-state, the carbonyl group of amino acid residue A6 is hydrogen bonded to the B6 amide hydrogen; and the A11 amide hydrogen is hydrogen bonded to the B4 carbonyl and loosely to B3 (Blundell et al., 1972; Baker et al., 1988). These hydrogen bonds occur within a single insulin molecule and are also displayed as NOE's in 2D-NMR studies (Hua & Weiss, 1991; Weiss et al., 1991). In the R_M-state of insulin, which is bound by phenol, the carbonyl group of A6 is hydrogen bonded to the hydroxyl hydrogen of phenol, and the amide hydrogen of A11 is hydrogen bonded to the hydroxyl oxygen of the phenol ligand (Derewenda et al., 1989). Via an unknown mechanism, the above-mentioned hydrogen bonding pattern is altered as phenol moves into its binding site and A-chain interactions with the B-chain N-terminus change. This rearrangement of the hydrogen bonding pattern in insulin is independent of interaction with residues of another monomer and may precipitate the formation of the R_M-state hexamer, as well as the R_I-state bound by cyclohexanol (see legend to Figure 12).

The CD spectra of the R_I-state of insulin resemble that observed by Wollmer et al. (1987) for insulin hexamers in the presence of *m*-cresol, and coordinated by Ni^{2+}, which cannot assume a tetrahedral coordination. Our results suggest that the spectral changes observed by Wollmer et al. may be due to the formation of additional α-helix with concomitant rearrangement of β-sheet structure. The finding that similar changes occur in metal-coordinated hexamers suggests that the R_I-state, or a similar conformation, may also be an intermediate in the hexameric $T_M \rightarrow R_M$ transition, i.e., $T_I \rightarrow T_M \rightarrow R_I \rightarrow R_M$.

Our results demonstrate an alternate conformation of insulin, in its monomeric and dimeric state, which has a characteristic extra α-helical region presumably at the N-terminus of the B-chain (R_I-state). We have shown that the B-chain of insulin is capable of large structural adjustments which might influence A-chain interactions as well. Conformational changes at the B-chain amino-terminus have been previously found to confer a different conformation upon the carboxy-terminus of the same chain in different crystal structures (Smith & Dodson, 1992; Ciszak & Smith, 1994), and accordingly these studies have observed similar changes in solution. The carboxy-terminus of the B-chain is largely conserved throughout evolution and is believed to be important in receptor binding (Tager, 1990a). It has also been well established that position B25 is important in insulin–receptor interactions (Nakagawa & Tager, 1986; cf. Tager, 1990b; Mirmira et al., 1991); and accordingly, structural adjustments which involve this position ($T_I \rightarrow R_I$ transition) may also be relevant in receptor binding. Most importantly, the attainment of the R_I-state by native insulin may be the first conformational change induced in monomeric insulin in solution. Such a large degree of structural variability demonstrates the array of possible conformations

that insulin is capable of sustaining. These results illustrate the interdependence of conformational changes in small proteins and may prove to be relevant to understanding how insulin alters its structure to assume its final receptor-bound state.

ACKNOWLEDGMENT

I thank Paul Rubinstein for the preparation of canine hepatocytes, Dr. Satoe H. Nakagawa for her expert advice and support, and Kwun-Hui Ho for technical assistance. I also thank Dr. Stephen C. Meredith and Dr. Donald F. Steiner for their assistance in the preparation of the manuscript.

NOTE ADDED IN PROOF

We would like to indicate that we are aware of the effects that particular buffers and pH may have on the structural adjustments in proteins, and subsequent experiments have demonstrated that perchlorate ions used in these studies reduce insulin β-sheet structure. However, this effect is only observed in the presence of dimeric/monomeric insulin plus ligand. This further strengthens the argument presented above that, in the R_I-state, changes in the NH_2-terminus affect the COOH-terminus and in a manner similar, but not identical, to that of the hexameric R_M-state.

REFERENCES

Baker, E. N., Blundell, T. L., Cutfield, J. F., Cutfield, S. M., Dodson, E. J., Dodson, G. G., Hodgkin, D. M. C., Hubbard, R. E., Isaacs, N. W., Reynolds, C. D., Sakabe, K., Sakabe, N., & Vijayan, N. M. (1988) *Philos. Trans. R. Soc. London B319*, 369−456.

Blundell, T., Dodson, G., Hodgkin, D., & Mercola, D. (1972) *Adv. Protein Chem. 26*, 279−402.

Bonnevie-Nielson, V., Polonsky, K. S., Jaspan, J. J., Rubenstein, A. H., Schwartz, T., & Tager, H. S. (1982) *Proc. Natl. Acad. Sci. U.S.A. 79*, 2167−2171.

Brader, M. L., Kaarsholm, N. C., Lee, R. W. K., & Dunn, M. F. (1991) *Biochemistry 30*, 6636−6645.

Chothia, C., Lesk, A. M., Dodson, G. G., & Hodgkin, D. C. (1983) *Nature 302*, 500−505.

Ciszak, E., & Smith, G. D. (1994) *Biochemistry 33*, 1512−1517.

Cutfield, J. F., Cutfield, S. M., Dodson, E. J., Dodson, G. G., Reynolds, C. D., & Vallely, D. (1981) in *Structural Studies on Molecules of Biological Interest* (Dodson, G. G., Glusker, J., & Sayre, D., Eds.) pp 527−546, Oxford University Press.

Derewenda, U., Derewenda, Z., Dodson, E. J., Dodson, G. G., Reynolds, C. D., Smith, G. D., Sparks, C., & Swenson, D. (1989) *Nature 333*, 594−596.

Derewenda, U., Derewenda, Z. S., Dodson, G. G., Hubbard, R. E. (1990) in *Handbook of Experimental Pharmacology* (Cuatrecasas, P., & Jacobs, S., Eds.) Vol. 92, pp 23−39, Springer-Verlag, Berlin and Heidelberg, Germany.

Derewenda, U., Derewenda, Z., Dodson, E. J., Dodson, G. G., Bing, X., & Markussen, J. (1991) *J. Mol. Biol. 220*, 425−433.

Dodson, E. J., Dodson, G. G., Hubbard, R. E., & Reynolds, C. D. (1983) *Biopolymers 22*, 281−291.

Eftink, M. R., & Ghiron, C. A. (1976) *J. Phys. Chem. 80*, 486−493.

Frank, B. H., & Veros, A. J. (1968) *Biochem. Biophys. Res. Commun. 32*, 155−160.

Goldman, J., & Carpenter, F. H. (1974) *Biochemistry 13*, 4566−4574.

Hua, Q., & Weiss, M. A. (1991) *Biochemistry 30*, 5505−5514.

Hua, Q. X., Shoelson, S. E., Kochoyan, M., & Weiss, M. A. (1991) *Nature 354*, 238−241.

Hua, Q. X., Shoelson, S. E., & Weiss, M. A. (1992) *Biochemistry 31*, 11940−11951.

Hua, Q. X., Ladbury, J. E., & Weiss, M. A. (1993) *Biochemistry 32*, 1433−1442.

Inouye, K., Watanabe, K., Tochino, Y., Kobayashi, M., & Shigeta, Y. (1981) *Biopolymers 20*, 1845−1858.

Lakowicz, J. R. (1983a) in *Principles of Fluorescence* Spectroscopy, pp 44−45, Plenum Press, New York.

Lakowicz, J. R. (1983b) in *Principles of Fluorescence* Spectroscopy, pp 345−347, Plenum Press, New York.

Lakowicz, J. R. (1983c) in *Principles of Fluorescence* Spectroscopy, pp 261−273, Plenum Press, New York.

Liang, D. C., Stuart, D., Dai, J. B., Todd, R., You, J. M., & Luo, M. Z. (1985) *Sci. Sin. 28*, 472−484.

Markussen, J., Jorgensen, K. H., Sorensen, A. R., & Thim, L. (1985) *Int. J. Peptide Protein Res. 26*, 70−77.

Mirmira, R. G., & Tager, H. S. (1989) *J. Biol. Chem. 264*, 6349−6354.

Mirmira, R. G., Nakagawa, S. H., & Tager, H. S. (1991) *J. Biol. Chem. 266*, 1428−1436.

Morihara, K., Ueno, Y., & Sakina, K. (1986) *Biochem. J. 240*, 803−810.

Nakagawa, S. H., & Tager, H. S. (1986) *J. Biol. Chem. 261*, 7332−7341.

Nakagawa, S. H., & Tager, H. S. (1991) *J. Biol. Chem. 266*, 11502−11509.

Nakagawa, S. H., & Tager, H. S. (1993) *Biochemistry 32*, 7237−7243.

Roy, M., Brader, M. L., Lee, R. W. K., Kaarsholm, N. C., Hansen, J. F., & Dunn, M. F. (1989) *J. Biol. Chem. 264*, 19081−19085.

Schwartz, G. P., Burke, G. T., & Katsoyannis, P. G. (1989) *Proc. Natl. Acad. Sci. U.S.A. 86*, 458−461.

Shoelson, S. E., Lee, J., Lynch, C. S., Backer, J. M., & Pilch, P. F. (1993) *J. Biol. Chem. 268*, 4085−4091.

Smith, G. D., & Dodson, G. G. (1992) *Proteins 14*, 401−408.

Smith, G. D., & Ciszak, E. (1994) *Proc. Natl. Acad. Sci. U.S.A. 91*, 8851−8855.

Steiner, D. F., Bell, G. I., & Tager, H. S. (1990) in *Endocrinology* (DeGroot, L. J., Ed.) pp 1263−1289, Saunders, Philadelphia.

Tager, H. S. (1990a) in *Handbook of Experimental Pharmacology* (Cuatrecasas, P., & Jacobs, S., Ed.) Vol. 92, pp 41−64, Springer-Verlag, Berlin and Heidelberg, Germany.

Tager, H. S. (1990b) in *Molecular Biology of Islets of Langerhans* (Okamoto, H., Ed.) pp 263−286, Cambridge University Press, Great Britain.

Thomas, B., & Wollmer, A. (1989) *Biol. Chem. Hoppe-Seyler 370*, 1235−1244.

Valdes, R., & Ackers, G. K. (1979) *Methods Enzymol. 61*, 125−142.

Weber, G. (1960) *Biochem. J. 75*, 335−345.

Weiss, M. A., Hua, Q. X., Lynch, C. S., Frank, B. H., & Shoelson, S. E. (1991) *Biochemistry 30*, 7373−7389.

Wollmer, A., Rannefeld, B., Johansen, B. R., Hejnaes, K. R., Balschmidt, P., & Hansen, F. B. (1987) *Biol. Chem. Hoppe-Seyler 368*, 903−911.

Wollmer, A., Rannefeld, B., Stahl, J., & Melberg, S. G. (1989) *Biol. Chem. Hoppe-Seyler 370*, 1045−1053.

BI9429389